EPJ Web of Conferences **305**, 00023 (2024) https://doi.org/10.1051/epjconf/202430500023
AOP2024

Refractive index and thickness analysis of planar interfaces by prism coupling technique

Paulo Lourenço [1,2*], *Yuri* Vygranenko[2], *Miguel* Fernandes[1,2], *Alessandro* Fantoni[1,2], and *Manuela* Vieira[1,2,3]

[1]IPL/ISEL/DEETC, Instituto Politécnico de Lisboa, Instituto Superior de Engenharia de Lisboa, Departamento de Engenharia Eletrónica e Telecomunicações e de Computadores, R. Conselheiro Emídio Navarro, 1949-014 Lisboa, Portugal
[2]CTS-UNINOVA and LASI, Caparica, Portugal
[3]NOVA School of Science and Technology, Caparica, Portugal

Abstract. Since 2022, various foundries are offering the manufacture of integrated photonic structures for the visible spectrum. As this technology continues to enter the market, there will be an increasing demand for accurate optical and dimensional characterization of these structures. To meet this demand, we have developed a highly precise optical characterization system based on the prism coupling technique, also known as m-lines spectroscopy, to investigate the optical properties of hydrogenated amorphous silicon nitride planar waveguides deposited by plasma-enhanced chemical vapor deposition. In this work, by combining visible spectroscopy with the prism coupling technique to excite modes that propagate resonantly in the waveguide via frustrated total internal reflection, using either parallel or perpendicularly polarized light beams, we were able to analyze the waveguide properties of silicon nitride thin films with an interfacial oxide layer. Furthermore, through numerical simulation of the bilayer structure, we calculate the waveguide's refractive index and thickness, and determine the characteristics of the interfaces in terms of refractive index and thickness.

1 Introduction

Approximately two decades after the midpoint of the last century, a reliable and highly precise technique for measuring the refractive index and thickness of transparent thin films [1]–[3] was developed. This technique commonly utilizes an optical setup known as the prism waveguide coupler. The basic components of this setup include a prism that is pressed against the thin film under analysis, which is typically deposited on an optical glass substrate. By controlling the pressure applied to the prism/film system, the air gap between the prism and the film can be adjusted, thereby influencing the coupling efficiency. The theoretical foundation of this method is based on the prism-waveguide coupler mode equations, which allow for the accurate determination of the refractive index and thickness of the transparent thin film.

Regarding the air gap dimension, the theoretical approach may be classified and treated as in the following waveguide systems:

- Slab waveguide mode equations: These consider an infinite air gap between the prism and the thin film [4], [5];
- Leaky waveguide mode equations: These assume the air gap is zero [6];
- Prism waveguide coupler mode equations: These allow for a variable air gap thickness, ranging from zero to infinity,

where the slab and leaky waveguide approaches represent specific cases of the more general prism waveguide mode equations.

To determine the refractive index and thickness of a transparent thin film, the synchronous directions corresponding to specific incidence angles at the prism's edge, which excite a propagating mode in the thin film via evanescent coupling, are experimentally obtained using a prism waveguide coupler setup. The thickness and refractive index of the transparent thin film can then be calculated by numerically solving the mode equations. In this work, we have combined the prism coupling technique with visible spectroscopy to determine the optical constants and thickness of thin films and developed an approach which enables the identification of the presence and thickness of an interfacial layer.

The Manifacier/Swanepoel method used in this study was initially developed by Manifacier et al. [7] and later refined by Swanepoel [8] for determining the optical constants and thickness of hydrogenated amorphous silicon thin films. This method, also known as the T-spectra method, is based on the transmission spectra of a transparent thin film under normal incidence. The complex refractive index and thickness of the sample are determined by analysing the interference fringes observed in the transmission spectra.

---

* Corresponding author: plourenco@deetc.isel.ipl.pt

Moreover, the T-spectra method provides insights into the optical uniformity of the transparent thin film. If the film is uniform, the interference effect produces a series of fringes in the transmission spectra, which can be used to determine the film's complex optical constants and thickness. However, the presence of an interfacial layer, or a graded refractive index within the film bulk, reduces the amplitude of these interference fringes and alters their peak values.

The refractive index and thickness results obtained in this work for the transparent thin film were verified using our software platform, Synopsys RSoft [9], through simulations of the structure discussed earlier and later in this document. This verification process also included determining the interfacial layer thickness by simulating the bilayer structure, and identifying the propagating modes for TE, and TM polarizations.

2 Experimental

The hydrogenated amorphous silicon nitride (a-SiN$_x$:H) thin films for this study were deposited on alkali-free glass substrates using a capacitively-coupled parallel-plate 13.56 MHz PECVD system. The gases used were SiH$_4$, NH$_3$ and H$_2$ at an SiH$_4$/H$_2$ dilution ratio of 1:9. The details on the deposition process have been reported elsewhere [10]. The optical transmission spectra were measured by a Shimadzu 3100 UV-Vis-NIR spectrophotometer.

Our optical setup for prism coupling measurements [11] comprises an angular actuator/motor, the Thorlabs PRM1-Z8, which is controlled by a Thorlabs K-Cube KDC101 controller connected to a PC. The photodetector placed adjacent to the prism's edge where the reflected beam is refracted. It is connected to a Rigol DM-3058 multimeter for signal measurements. By incorporating a polarizer, the Thorlabs LPVIS100, between the laser diode and the prism, we can monitor parallel and perpendicular polarized incoming beams, enabling the selective excitation of transverse magnetic (TM) or transverse electric (TE) modes.

The entire system is controlled via USB connection to the PC, which oversees both the angular displacement of the prism and data acquisition from the photodetector through the multimeter. A developed C# application on the PC manages various functions of the angular actuator/motor, and it also handles the display and storage of the photodetector's signal.

3 Results and Discussion

Fig. 1 shows the transmission spectra of the a-SiN$_x$ thin film used in our study. The spectra were measured on the day of sample preparation and three years later when the sample was used for prism coupling experiments. Both spectra show similar interference fringes; however, the peaks of the later curve are above the transmittance of the glass substrates. This is indicative of films with a graded refractive index. We assume that the SiO$_x$ layer grows permanently over time due to unavoidable nitride surface oxidation in air [12].

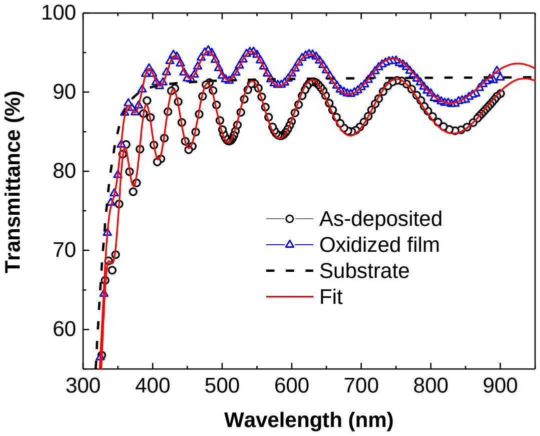

Fig. 1. Transmission spectra of the a-SiNx:H thin film measured immediately after deposition and 3 years later.

The film thickness of 1068 nm and the n&k dispersion curves shown in Fig. 2 were obtained from the spectrum of the as-deposited film using the Swanepoel method [8]. Similar optical constants for a-SiN$_x$:H have been reported elsewhere [13]. These data were utilized to simulate the fitting curves presented in Fig. 1. The Transfer Matrix Method (TMM) was employed to simulate the transmission spectrum of the glass/SiN$_x$/SiO$_2$ bilayer at $n_{SiO2} = 1.5$ [14,15]. The best fit was achieved with SiN$_x$ and SiO$_2$ layer thicknesses of 1012 nm and 72 nm, respectively.

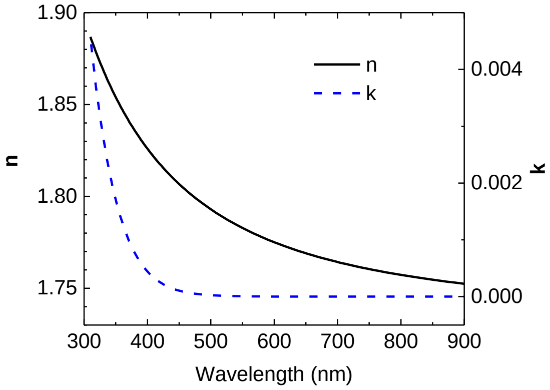

Fig. 2. Refractive index and extinction coefficient curves for an a-SiN$_x$:H thin film.

Fig. 3 displays the processed signals measured under TE and TM light polarizations at a wavelength of 656 nm, revealing three resonance peaks at both polarizations corresponding to mode orders 0, 1, and 2. The obtained modal indices, alongside the calculated refractive index (n_f) and film thickness (d) (combinations mode 0 & mode 1 and mode 0 & mode 2, have been considered), are listed in Table 1. The n_f values, ranging from 1.766 to 1.770, are consistent with the refractive index n(656nm) = 1.768 obtained by spectroscopy. The average thickness values are 1023 nm and 1012 nm for TM and TE modes, respectively, with the latter matching the thickness of the SiN$_x$ layer calculated from the observed resonances.

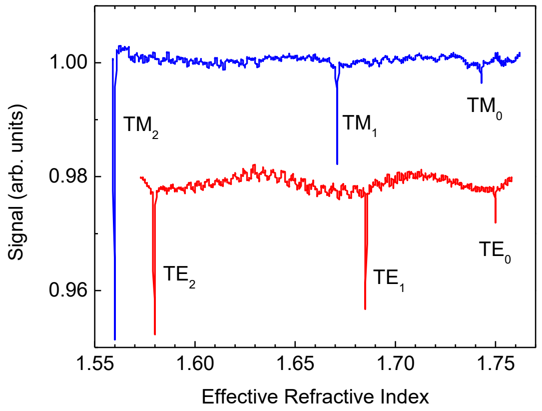

Fig. 3. Experimental dependences for excitation of TM and TE modes in the a-SiN$_x$:H waveguide.

Table 1. Measured modal refractive indices and calculated refractive index and film thickness.

Modes	0	1	2	n_f	d [nm]
TM	1.7425	1.671	-	1.767	1019
TM	1.7425	-	1.559	1.766	1027
TE	1.7496	1.685	-	1.770	1009
TE	1.7496	-	1.579	1.770	1014

The following equations were used to calculate n_f and d for TE and TM modes [1]:

$$\sqrt{\frac{n_f^2-N_i^2}{n_f^2-N_j^2}}=\frac{arctan\sqrt{\frac{N_i^2-n_a^2}{n_f^2-N_i^2}}+arctan\sqrt{\frac{N_i^2-n_s^2}{n_f^2-N_i^2}}+m_i\pi}{arctan\sqrt{\frac{N_j^2-n_a^2}{n_f^2-N_j^2}}+arctan\sqrt{\frac{N_j^2-n_s^2}{n_f^2-N_j^2}}+m_j\pi}, \quad (1)$$

$$d=\frac{\lambda}{2\pi\sqrt{n_f^2-N_m^2}}\left[arctan\sqrt{\frac{N_m^2-n_a^2}{n_f^2-N_m^2}}+arctan\sqrt{\frac{N_m^2-n_s^2}{n_f^2-N_m^2}}+m\pi\right] \quad (2)$$

$$\sqrt{\frac{n_f^2-N_i^2}{n_f^2-N_j^2}}=\frac{arctan\frac{n_f^2}{n_a^2}\sqrt{\frac{N_i^2-n_a^2}{n_f^2-N_i^2}}+arctan\frac{n_f^2}{n_s^2}\sqrt{\frac{N_i^2-n_s^2}{n_f^2-N_i^2}}+m_i\pi}{arctan\frac{n_f^2}{n_a^2}\sqrt{\frac{N_j^2-n_a^2}{n_f^2-N_j^2}}+arctan\frac{n_f^2}{n_s^2}\sqrt{\frac{N_j^2-n_s^2}{n_f^2-N_j^2}}+m_j\pi}, \quad (3)$$

$$d=\frac{\lambda}{2\pi\sqrt{n_f^2-N_m^2}}\left[\begin{matrix}arctan\frac{n_f^2}{n_a^2}\sqrt{\frac{N_m^2-n_a^2}{n_f^2-N_m^2}}+\\ arctan\frac{n_f^2}{n_s^2}\sqrt{\frac{N_m^2-n_s^2}{n_f^2-N_m^2}}+m\pi\end{matrix}\right], \quad (4)$$

where $k_0 = 2\pi / \lambda$, λ is the radiation wavelength, n_a the refractive index of air, n_s the refractive index of substrate, N_m the modal index, and m is the mode order.

Equations (1) to (4) are valid for the optically uniform film, and their use for a film with a graded index interface may result in significant errors. To address this, we simulated the glass/SiN$_x$/SiO$_2$ structure using RSoft's mode solver. Fig. 4 displays the calculated modal refractive indices for TE and TM modes as a function of the SiO$_2$ layer thickness. The modelling was conducted while keeping the combined thickness of the SiN$_x$/SiO$_2$ bilayer constant at 1000 nm. We then processed these data using equations (1 – 4) to determine the values of n_f and d. The obtained refractive index values matched exactly with the refractive index of the SiN$_x$ layer used in the mode solver, while the thickness varied depending on the SiO$_2$ layer thickness. Figure 5 shows the relationship between the SiN$_x$ core layer thickness and the SiO$_2$ layer thickness. In this figure, the reference line (dash-dot line) indicates the model parameter for the SiN$_x$ layer thickness. This suggests that the presence of an interface layer can lead to an overestimation of the core layer thickness. This procedure predicts an error of approximately 23 nm when the interface layer is 72 nm thick. Additionally, the difference between the TM and TE thicknesses increases linearly at a rate of 0.13, predicting a thickness difference of 9.4 nm at a SiO$_2$ thickness of 72 nm, which aligns well with experimental results. The SiO$_2$ layer thickness can also be estimated in reverse.

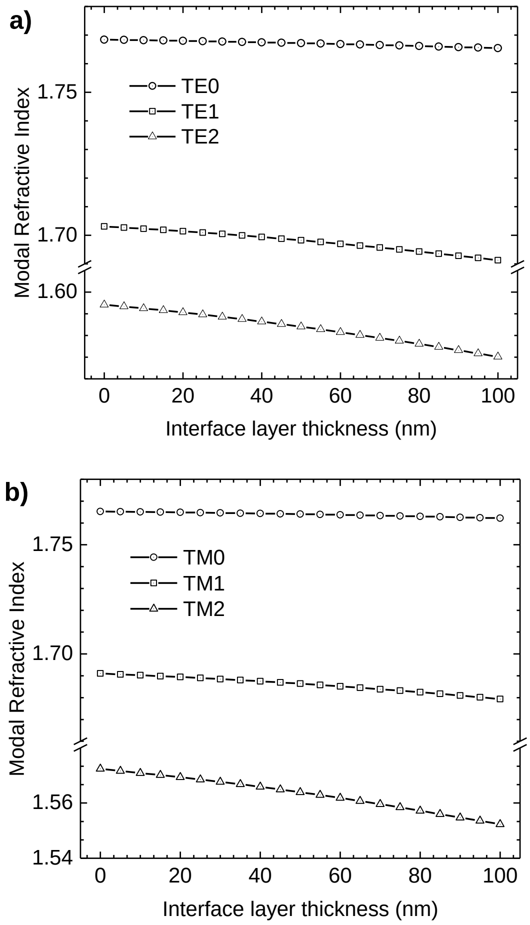

Fig. 4. Simulated modal refractive indices for (a) TE and (b) TM polarizations versus the SiO$_2$ layer thickness.

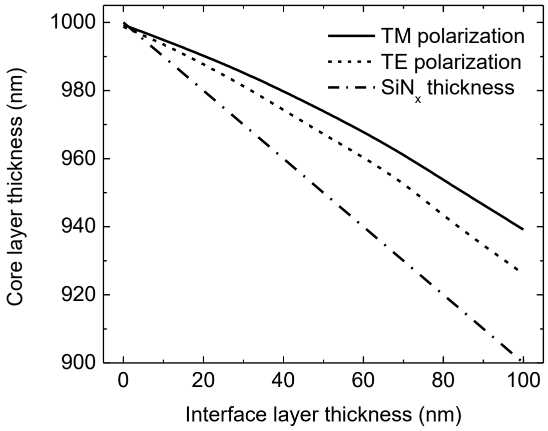

Fig. 5. Calculated SiN$_x$ core layer thickness versus the SiO$_2$ layer thickness. The reference line (dash-dot line) indicates the SiN$_x$ layer thickness in the numerical model.

4 Conclusions

We have applied the prism coupling technique to thin films with a capping interface layer. Numerical simulations demonstrate that the refractive index of the a-SiN$_x$:H film with an interfacial oxide layer can be accurately determined using the propagation equations, which are obtained for a single-core waveguide with abrupt interfaces. However, the thickness of the film may be overestimated depending on the thickness of the oxide layer. This thickness overestimation can be corrected by numerically modelling the bilayer structure and analysing the experimental data.

Acknowledgments

This research was supported by Portuguese national funds provided by the Portuguese FCT program, Centre of Technology and Systems (CTS) UIDB/00066/2020/ UIDP/00066/2020, by FCT project ASER-META 2022.07694.PTDC and by IPL project IPL/IDI&CA2023/ DETPREC_ISEL. A special word of appreciation to BSc. Jorge Fidalgo for his contributions in this work, namely concerning the design and implementation of the mechanical fixtures in the optical setup.

References

[1] P. K. Tien, R. Ulrich, and R. J. Martin, “Modes of propagating light waves in thin deposited semiconductor films,” *Appl. Phys. Lett.*, vol. 14, no. 9, pp. 291–294, 1969, doi: 10.1063/1.1652820.

[2] P. K. Tien and R. Ulrich, “Theory of Prism–Film Coupler and Thin-Film Light Guides,” *J. Opt. Soc. Am.*, vol. 60, no. 10, pp. 1325–1337, 1970, doi: 10.1364/josa.60.001325.

[3] R. Ulrich, “Theory of the Prism–Film Coupler by Plane-Wave Analysis,” *J. Opt. Soc. Am.*, vol. 60, no. 10, p. 1337, Oct. 1970, doi: 10.1364/JOSA.60.001337.

[4] R. Ulrich and R. Torge, “Measurement of Thin Film Parameters with a Prism Coupler,” *Appl. Opt.*, vol. 12, no. 12, p. 2901, 1973, doi: 10.1364/ao.12.002901.

[5] D. Marcuse, *Theory of Dielectric Optical Waveguides*. Elsevier, 1991.

[6] R. T. Kersten, “A new method for measuring refractive index and thickness of liquid and deposited solid thin films,” *Opt. Commun.*, vol. 13, no. 3, pp. 327–329, 1975, doi: 10.1016/0030-4018(75)90112-1.

[7] J. C. Manifacier, J. Gasiot, and J. P. Fillard, “A simple method for the determination of the optical constants n, k and the thickness of a weakly absorbing thin film,” *J. Phys. E.*, vol. 9, no. 11, pp. 1002–1004, Nov. 1976, doi: 10.1088/0022-3735/9/11/032.

[8] R. Swanepoel, “Determination of the thickness and optical constants of amorphous silicon,” *J. Phys. E.*, vol. 16, no. 12, pp. 1214–1222, Dec. 1983, doi: 10.1088/0022-3735/16/12/023.

[9] RSoft, “Synopsys RSoft Solutions.” https://www.synopsys.com/optical-solutions/rsoft.html (accessed Jul. 30, 2024).

[10] G. Lavareda *et al.*, “Dependence of optical properties on composition of silicon carbonitride thin films deposited at low temperature by PECVD,” *J. Non. Cryst. Solids*, vol. 551, no. July 2020, p. 120434, Jan. 2021, doi: 10.1016/j.jnoncrysol.2020.120434.

[11] P. Lourenço *et al.*, “Determining Thin Film Characteristics by Prism Coupling Technique,” In Doctoral Conference on Computing, Electrical and Industrial Systems, pp. 337–347. Cham: Springer Nature Switzerland, 2024.

[12] S. I. Raider, "Surface Oxidation of Silicon Nitride Films," Journal of The Electrochemical Society, vol. 123, no.4, 560, 1976, doi:10.1149/1.2132877.

[13] G. Lavareda, Y. Vygranenko, A. Amaral , P. Brogueira, “Effect of dehydrogenation on optical constants of silicon nitride thin films”, Optical Materials, vol. 145, no. 8, 114480, Nov. 2023, doi: 10.1016/j.optmat.2023. 114480.

[14] C.C. Katsidis, D.I. Siapkas, General transfer-matrix method for optical multilayer systems with coherent, partially coherent, and incoherent interference, Appl. Opt., vol. 41, pp. 3978–3987, 2002, doi: 10.1364/AO.41.003978.

[15] Y. Vygranenko, G. Lavareda, M. Fernandes, M. Vieira, “Characterization and modeling of a-Si:H-based n-i-p photodiodes with protocrystalline silicon p-layers,” Thin Solid Films, vol. 784, no. 14, Nov. 2023, doi: 10.1016/j.tsf.2023.140072.